Part I

Concepts of Self-Cleaning Surfaces

1

Superhydrophobicity and Self-Cleaning

Paul Roach[1] *and Neil Shirtcliffe*[2]
[1]*Institute for Science and Technology in Medicine, Guy Hilton Research Centre, Keele University, UK*
[2]*Faculty of Technology and Bionics, Hochschule Rhein-Waal, Germany*

One of the ways that surfaces can be self-cleaning is by repelling water so effectively that water-borne contaminants cannot attach – by being superhydrophobic. This is demonstrated particularly well by the Indian Lotus, *Nelumbo nucifera*, which has leaves that remain clean in muddy water. The leaves can be cleaned of most things by drops of water, an effect that has been patented and used in technical systems [1].

1.1 Superhydrophobicity

1.1.1 Introducing Superhydrophobicity

Superhydrophobicity is where a surface repels water more effectively than any flat surface, including one of PTFE (Teflon®). This is possible if the surface of a hydrophobic solid is roughened; the liquid/solid interfacial area is increased and the surface energy cost increases. If the roughness is made very large, water drops bounce off the surface and it can become self-cleaning when it is periodically wetted. To understand more about this type of self-cleaning it is necessary to consider how normal surfaces become wetted and become dirty. The effect has been a focus of much recent research and has been reviewed recently [2–7]. A good mathematical explanation can be found in a recent book chapter by Extrand [8].

Self-Cleaning Materials and Surfaces: A Nanotechnology Approach, First Edition. Edited by Walid A. Daoud.

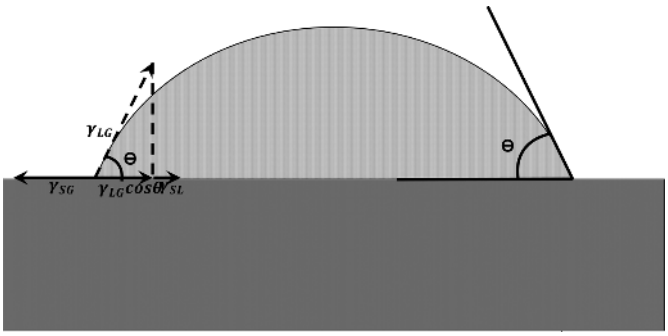

Figure 1.1 *Cross-section of a drop on a flat surface with the contact angle θ. Contact angles also form at the edge of larger pools of water, in tubes, at bubbles on underwater surfaces and any other configuration where a liquid interface meets a solid.*

1.1.2 Contact Angles and Wetting

When a liquid rests on a surface the "contact angle" is measured through the droplet between the solid/liquid and liquid/air interfaces. The equilibrium angle that forms is known as Young's angle after a theory proposed by Young, but not actually formulated in his work [9]. Young's equation can be considered as a force balance of lateral forces on a contact line. In a perfect system the contact line cannot sustain any lateral force, so will always move to a position where the forces balance. This is achieved mathematically by taking the components of each force in the plane of the surface, at right angles to the contact line, as shown in Figure 1.1.

$$\gamma_{\mathrm{SG}} = \gamma_{\mathrm{SL}} + \gamma_{\mathrm{LG}} \cos\theta \tag{1.1}$$

where γ is the interfacial tension and the subscripts refer to solid, liquid and gas, for example, γ_{SL} is the interfacial tension between solid and liquid.

Young's equation can also be derived from the surface and interfacial energies and their changes. The contact angle is an important measure of the interaction between the three phases, one solid, a liquid and another fluid, which may be a liquid or a gas. For small drops on a flat surface the drops form spherical caps, spheres intersecting the surface. External factors, such as electric fields, may also influence the drop shape, with gravity playing a role in distorting larger droplets. At the contact line the angle tends to the Young angle except when the contact line is moving relatively rapidly. In most systems there is a certain uncertainty in contact angle known as contact angle hysteresis.

1.1.3 Contact Angle Hysteresis

In practice the equilibrium angle is often difficult to measure because there are a small range of angles on every surface that are stable. These are often described as local energy minima close to the global energy minimum. In practice the contact line therefore often behaves as though it were fixed over a small range of angles close to the equilibrium angle [10]. Traditionally, the equilibrium contact angle was approached by vibrating the surface to supply the energy for the drop to escape the local minima. Although the static angle can

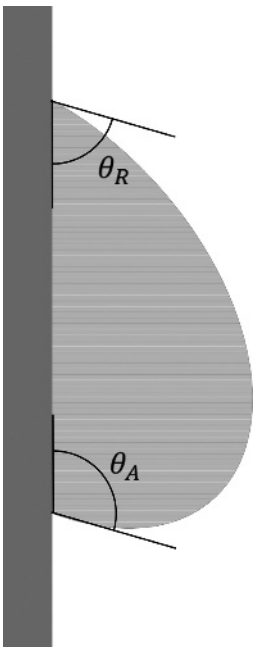

Figure 1.2 *A drop on a vertical surface sliding slowly with advancing angle at the front and receding angle at the back, in practice geometrical factors and speed of movement will change the angles away from the actual advancing and receding angles.*

vary, the contact line begins to move at a certain angle when the liquid front is advanced and at a different angle when it recedes. These values are simpler to measure so it is often the greatest stable angle and the lowest stable angle that are measured, known as the advancing and receding angles. The angles commonly quoted are those measured at a very low speed as the measured angles are affected by the speed of motion of the contact line. This is usually carried out by injecting liquid slowly into a drop and removing it again. Often the advancing and receding angles are of more practical use than the equilibrium angle, although the equilibrium value can be used to derive surface energies. It is sometimes possible to determine the equilibrium angle if both advancing and receding angles are measured. This still assumes that hysteresis is not very large and the surface is reasonably flat [11].

The difference between the advancing and receding angles, or rather the difference between the cosines of the angles governs whether liquids will stick to a surface or slide or fall off. A drop on a vertical sheet can have the advancing angle at the bottom and the receding angle at the top without moving (Figure 1.2). Surfaces with low hysteresis allow drops to slide over them whatever the equilibrium contact angle. The energy required for a drop to move can be calculated as [12],

$$F = \frac{1}{2\pi r}\gamma_{\mathrm{LG}}(\cos\theta_{\mathrm{rec}} - \cos\theta_{\mathrm{adv}}) \tag{1.2}$$

where r is the base radius of the drop. The contact angle itself enters the equation in two ways: first the cosine function enhances differences near 90°; secondly the value of the contact radius r, for a given volume depends upon the contact angle.

Furmidge calculated the angle of tilt, α, required in order for a drop to slide [13],

$$\frac{mg \sin \alpha}{w} = \gamma_{LG} (\cos \theta_{rec} - \cos \theta_{adv}) \tag{1.3}$$

where w is the width of the drop.

Measurement of the force required to remove drops from surfaces and tilting angles shows the general trend is correct but some differences can be measured, particularly for softer surfaces. Going back to Young's equation, if the force balance approach is used, the surface tension components in the plane of the solid are balanced to give the contact angle, but this leaves a vertical force on the surface, depending upon contact angle. Theories by de Gennes and Shanahan [14] and experiments on soft materials suggest that this force distorts the surface, generating a ring like an atoll around the base of the drop and increasing the force restraining the drop from sliding on the surface. Of course the drop profile is also far from a circle if hysteresis is significant, particularly for large drops (for example that shown in Figure 1.2).

The receding angle (and liquid properties) controls whether a drop falls off an inverted surface, the advancing angle is not involved as it is never reached in this case.

The work needed to pull a liquid from a surface has been reported to be determined by [15, 16].

$$W = \gamma_{LG} (1 + \cos \theta R) \tag{1.4}$$

1.1.4 The Effect of Roughness on Contact Angles

1.1.4.1 Fully Wet Surfaces; Wenzel's Equation

As the roughness is increased the water initially wets the entire surface, as shown in Figure 1.3b, the increasing surface area of the interface means that the advancing contact angle on a surface with a flat contact angle of greater than 90° increases, whereas that of one below 90° decreases. A surface with exactly 90° contact angle would show no effect of roughness. This type of wetting can, therefore, be considered to be an amplification of the properties of the surface by the roughness. The contact angle of a rough surface of this type can be calculated using Wenzel's equation [17], which modifies the cosine of the angle by the specific surface area, r , the amount of times the surface is larger than a flat surface of the same size. The subscript e has been used to highlight that usually the equilibrium contact angle is considered as opposed to the receding or advancing contact angles introduced in Section 1.1.3.

$$\cos \theta_{rough} = r \cos \theta_e \tag{1.5}$$

The amplification of both hydrophilicity and hydrophobicity arises from the change in sign of cosθ at 90°.

1.1.4.2 Bridging the Roughness; Cassie and Baxter's Equation

If the surface is roughened it eventually becomes energetically favourable for the liquid to sit on the top of the roughness and reduce the area of the interface, as shown in Figure 1.3c.

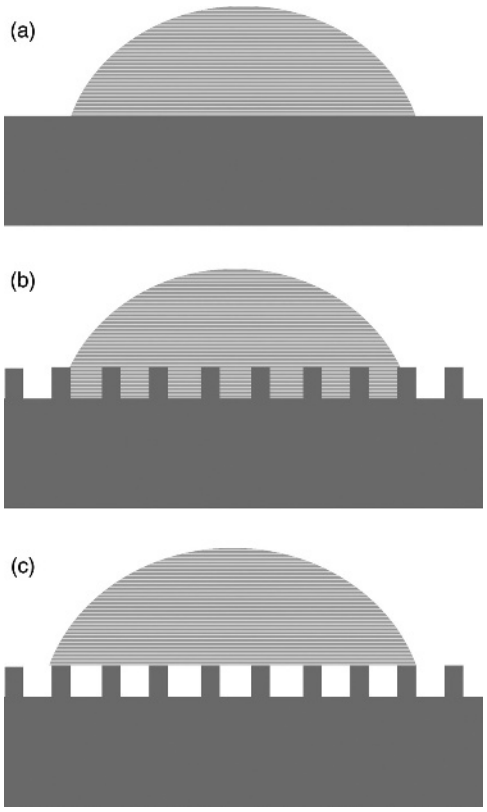

Figure 1.3 *Wetting on flat and rough surfaces: (a) flat, (b) rough, Wenzel case; (c) Cassie and Baxter case.*

In this case the state approaches that of a liquid on a flat surface with domains of different contact angles but where one of the materials is the second fluid (in this example air).

The simplest expression for the contact angle on a surface of this type was formulated in 1944 by Cassie and Baxter [18]. This considers the cosine of the angle to be the mean of the cosines of both contributing surfaces weighted by their relative areas, denoted by f, the fraction of the interface that is solid.

$$\cos\theta_{\text{rough}} = f\cos\theta_{\text{e}} + (f - 1) \tag{1.6}$$

This equation considers both the solid/liquid and the liquid/gas interfaces to be planar, which is only the case if the surface consists of equal height flat-topped pillars. The original Cassie and Baxter paper allowed for deviations from this by effectively using Wenzel's equation for the wetted part and allowing changes in the effective roughness with penetration. The main problem with this approach is that it is often difficult to determine where the liquid/solid interface lies.

1.1.5 Where the Equations Come From

Both Wenzel and Cassie–Baxter equations can be derived from forces at the contact line or from interfacial areas. Using the interfacial areas effectively considers a minimisation of the surface energy of the system. A force balance argument is equivalent, but considers the surface energy from the forces it generates and creates conceptual difficulties when sharp corners are considered [19].

Because of the increased interfacial area in the Wenzel case and the decrease in interfacial area in the Cassie–Baxter case the hysteresis observed increases in the Wenzel state and decreases in the Cassie–Baxter state, giving rise to low water adhesion in the Cassie–Baxter state [20].

1.1.5.1 Flat Surfaces

Consider a liquid on a surface with a contact line at a contact angle; if we allow this line to move by an infinitesimal amount and assume that it will move in this manner until it reaches an energy minimum the energy minimum can be defined as the position where moving the contact line by a small amount does not change the interfacial energy. This does assume that there is a single minimum in the energy profile – a reasonable assumption for a flat surface.

The energy change for moving forward a small amount is illustrated in Figure 1.4. The area of the liquid/fluid interface changes by $\Delta A \cos\theta$, the solid liquid interface changes area by ΔA and replaces or is replaced by the same amount of solid surface (depending on the direction of motion). The total change in surface free energy, ΔF, accompanying an advance of the contact line is therefore,

$$\Delta F = (\gamma_{SL} - \gamma_{SG})\,\Delta A + \Delta A \gamma_{LG} \cos\theta \tag{1.7}$$

If we set the change in free energy to zero we will find the minimum or maximum of the expression, in this case because we are starting close to the global minimum we will approach that. The result can be rearranged to form Young's equation.

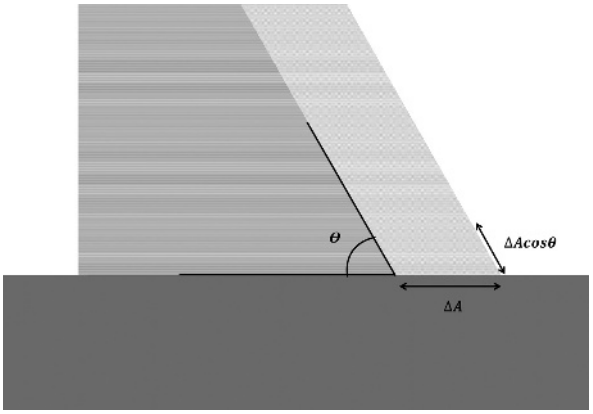

Figure 1.4 *Contact angle and surface free energy.*

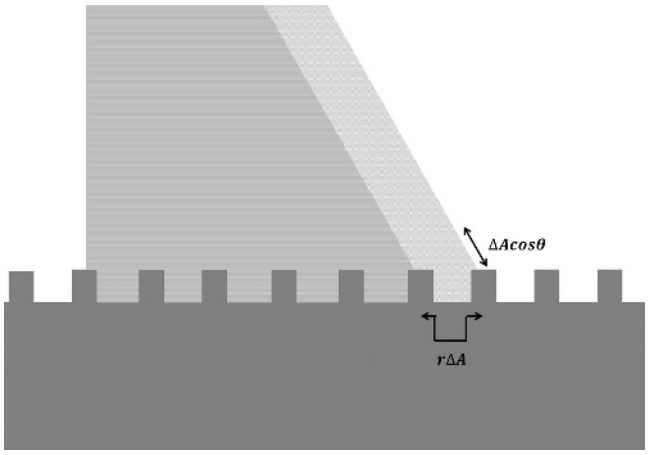

Figure 1.5 *Wenzel wetting.*

On a flat surface this treatment is equivalent to a force balance, but on rough surfaces this surface free energy treatment averages over a period of the roughness or a representative area. Unlike a force balance there are no difficulties when the contact line meets the corner of a feature and the intrinsic assumption that the contact line is always on a representative proportion of the surface is slightly more obvious. In cases where this is not true, for patterns that are large compared with the size of the drop, when the contact line can sit on one part of the pattern or when the pattern is anisotropic (e.g., parallel grooves) the approach cannot be applied without some modification.

1.1.5.2 Wenzel Case

For a rough surface where the liquid wets into the rough features (Figure 1.5), the treatment is the same as the flat surface but the surface areas of both the solid/liquid and the solid/vapour interfaces associated with the advance of the contact line are increased by a factor, r, the specific surface area of the rough surface at the contact line. In other words the number of times larger the area is than if it were flat. The roughness factor compares the rough surface to a two-dimensional surface of the same size and is, therefore, better served by this surface energy treatment. When the new values of the surface energies are treated in the same way as before the following expressions result,

$$\Delta F = (\gamma_{SL} - \gamma_{SG})\, r\, \Delta A + \Delta A \gamma_{LG} \cos\theta \tag{1.8}$$

$$\text{If } \Delta F = 0 \text{ then } \cos\theta = \frac{(\gamma_{SL} - \gamma_{SG}) r\, \Delta A}{\Delta A \gamma_{LG}} \tag{1.9}$$

This can be substituted into Young's equation to give Wenzel's equation.

1.1.5.3 Cassie–Baxter Case

To consider only bridging wetting we can imagine flat-topped pillars with water bridging the gaps between with horizontal menisci, as shown in Figure 1.6. In this particular

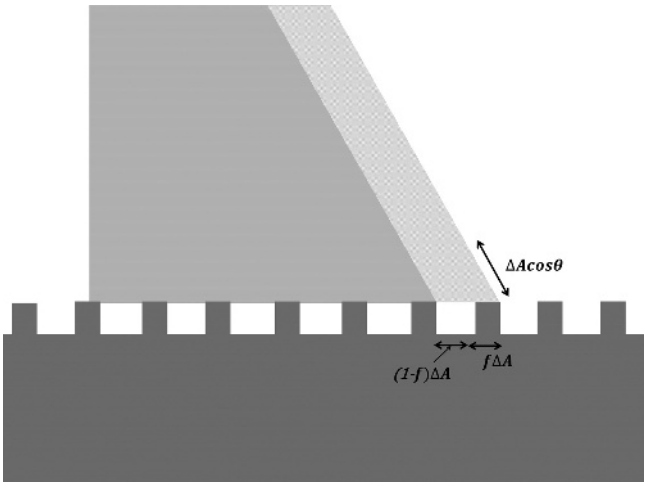

Figure 1.6 *The Cassie and Baxter case.*

configuration the surface area of the base of the water is the same as it would be on a flat surface.

Again the air/liquid interface at the top of the drop is unaffected by the roughness, the lower part advances over a combination of fluid (air) and solid, the interfacial area, A, can be divided into two components and these assigned to the solid or the fluid interface. The proportions of these two components are determined by the shape of the surface, in this case the relative areas of the tops of the pillars to the gaps.

The surface free energy can be minimised as before giving:

$$\Delta F = (\gamma_{SL} - \gamma_{SG})\, f \Delta A + (1 - f)\, \Delta A \gamma_{LG} + \gamma_{LG} \Delta A \cos\theta \tag{1.10}$$

and, again, with substitution into Young's equation it becomes reduced to the form of Cassie and Baxter's equation;

$$\cos\theta_{rough} = f \cos\theta_e + (f - 1) \tag{1.11}$$

It can be seen that the observed contact angle on this type of surface is intermediate between the liquid/solid contact angle and the liquid/fluid contact angle. If the second fluid is air or another gas the contact angle will always increase, even if the surface is hydrophilic. The reverse situation can be imagined where the pores at the surface are pre-filled with the same liquid as the drop, in this case the contact angle will decrease, even if the surface is repellent to the liquid. On hydrophilic surfaces this situation can arise when a film of liquid spreads through the roughness of the surface before the macroscopic drop spreads. The same equation can be used for flat surfaces with areas of different contact angle as long as they are distributed well. As mentioned above the original Cassie and Baxter paper considered the combined effect of these two situations.

1.1.5.4 Important Considerations

There has been some criticism of these equations, but these can also be interpreted as criticism of their misuse [21–24]. Both equations require a set of assumptions to be true (or at least locally true) for them to apply.

First, there is a requirement that the pattern of roughness or chemistry is arranged so that the contact line is always on the average of all parts of the structures. This is implicit in the treatments above where always an entire cycle of roughness (or chemical pattern) is taken. This requirement is broken if the pattern allows the contact line to arrange itself so that it is mostly on one type of the surface. This is particularly evident in grooved surfaces where the contact angles parallel and perpendicular to the grooves are different. Perpendicular to the grooves the expected angles form, whilst parallel to the groove direction a cyclic change is observed as the contact line moves over the peaks and troughs. Similar problems arise from other pattern geometries. Another way this requirement can be broken is if the size of the patterned features becomes large enough such that the contact line bends to reduce the interfacial energy of the liquid.

$$\kappa^{-1} = \sqrt{\frac{\gamma_{\mathrm{LG}}}{\rho g}} \tag{1.12}$$

The capillary length (Eq. 1.12) describes the general size where gravity will have a larger effect than surface tension on a drop of liquid. As can be seen the quantities compared are the surface tension (γ_{LG}) and the effect of gravity on the liquid through density(ρ) and gravity (g). For water on our planet this critical length is 2.73 mm; drops of radius much smaller than this, typically a tenth of this size, are almost spherical. In the same way the meniscus bridging two features will be distorted by gravity and this can be considered to become significant as the gaps reach a tenth of the capillary length. Structures larger than this can distort the contact line as they influence it via interfacial tension.

Secondly, as the thought experiment that generates the equations considers small movements from the equilibrium position the state of a liquid is only determined by the surface near the contact line. This is a long-winded way of stating that a drop on a hydrophobic surface will not spontaneously jump to a hydrophilic surface unless the contact line intersects both surfaces. It means that the solid/liquid interfacial area under the drop but away from the contact line is largely irrelevant when determining the contact angle, but if there are differences these will be revealed if the contact line moves over the surface – if a drop slides over the surface for example.

1.1.6 Which State Does a Drop Move Into?

As the Wenzel type of wetting is very different from Cassie and Baxter bridging wetting it is important to know which surface will end up in which state. Initial attempts to predict which state a surface would go into from Cassie–Baxter and Wenzel's equations met with mixed success. Even when the surface allows this type of comparison it is only possible from the equations above to find which of the states has the lowest energy minimum. Some theoretical treatments of the transition do exist and have shown success predicting experiments. In the simplest the energy levels of both states and those of intermediate states are calculated to determine which states are lowest in energy. More complicated ones attempt to discover when a water drop on the surface can become trapped in one

state or the other. In many experimental cases the small-scale roughness of the surface is difficult to measure, preventing this type of detailed calculation [25–27]. If a drop is placed onto the surface it is likely to start in the Cassie–Baxer state and may become trapped there even if the Wenzel state has a lower energy. Conversely, if water condenses onto a superhydrophobic surface it initially wets inside the roughness so generally starts in the Wenzel state and almost always becomes trapped there [28].

1.2 Self-Cleaning on Superhydrophobic Surfaces

1.2.1 Mechanisms of Self-Cleaning on Superhydrophobic Surfaces

Self-cleaning superhydrophobic surfaces first received attention when a paper was published on the Lotus leaf [29]. Lotus leaves remain clean in muddy water because of the way their surfaces are structured and water repellent. The leaves are strongly superhydrophobic and, although they collect particles of dust, they are fully cleaned by rain.

One of the mechanisms for self-cleaning, and that initially suggested for the lotus leaf, depends on how the water drop moves. A drop on a surface with high contact angle and low contact angle hysteresis, usually a bridging super-hydrophobic surface, can roll instead of sliding. This type of motion allows the drop to collect more of the particles at the surface of the solid compared to the usual sliding mechanism.

The question that then arises is why a rolling drop should collect hydrophobic particles from a superhydrophobic surface.

Particles, even hydrophobic ones, are strongly attached to a liquid/gas interface. If the particle is modelled as a sphere its lowest energy configuration is when it is located in the interface; partially immersed so that the local contact angle can be the equilibrium contact angle. The energy of attachment of a particle on a liquid interface can be calculated by comparing the surface energies of three possibilities, the particle away from the liquid, the particle at its equilibrium position in the interface and the particle inside the liquid. For a hydrophobic particle and water the third case will not be the lowest in energy so we can consider the energy change from the particle resting in air to being held at the interface.

When a spherical particle of radius R and contact angle θ_e attaches to a liquid interface the angle between the surfaces is the contact angle (Figure 1.7). The area of the sphere that becomes wetted can be described by Eq. (1.13), this is both the solid/gas interface that is lost and the solid/liquid interface gained. The liquid also loses some interface, the circular

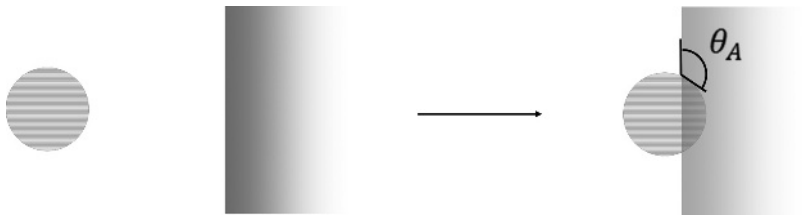

Figure 1.7 *A hydrophobic, spherical particle moving from the air to a position in a water interface where it has its contact angle with the liquid.*

patch that is now covered by the particle, given by Eq. (1.14) (R_s being the radius of the sphere).

$$2\pi R_S^2 (1 + \cos\theta_e) \tag{1.13}$$

$$\pi R_S^2 \sin^2\theta_e \tag{1.14}$$

The change in surface energy can therefore be calculated as:

$$\Delta F = 2\pi R_S^2 (1 + \cos\theta_e)(\gamma_{SL} - \gamma_{SV}) - \pi R_S^2 \sin^2\theta_e \gamma_{LG} \tag{1.15}$$

Substituting with Young's equation, Eq. (1.1) gives

$$\Delta F = -\gamma_{LG}\pi R_S^2 (1 + \cos\theta_e)^2 \tag{1.16}$$

As can be seen from the equation unless the equilibrium contact angle is 180° or 0° for a particle moving into the liquid it is always energetically favourable to attach a sphere to the interface. Very small particles may obtain enough energy from Brownian motion to escape. As the mass increases with radius cubed and the surface energy with radius squared, large particles can eventually become heavy enough to detach by gravity.

This explains why most particles should adhere to a passing droplet, but not why a rolling drop should be more efficient at removing them.

Examination of the rear edge of the drop as it pulls off the surface reveals some of the possible mechanisms for self-cleaning.

On a flat or a rough Wenzel-type surface the liquid wets the whole surface and the contact line slides over it as it retreats. As the line reaches a particle at the surface it moves over the particle, exerting little or no upward force as it is pinned on the surface to both sides of the particle (Figure 1.8a). On a bridging Cassie–Baxter surface when the contact line reaches the particle it can detach from the features around the particle but remain attached to it as it is a little higher. This allows considerable upward force to be exerted on the particle by the liquid, which could dislodge it (Figure 1.8b).

If we consider that a thin film may be left on the surface after the drop has passed this alters the situation a little. On a flat or Wenzel surface the interfaces of the drop are being lost at its rear and regenerated at the front, like a slug leaving a trail (Figure 1.8c). In this case any particles in the upper or lower interface will be dumped back onto the surface when the film evaporates, unless there is a very large flow carrying the particles away. Therefore, nearly all particles will return to their starting positions after the drop has passed. For the Cassie–Baxter bridging case leaving a water film, each interacting peak will spawn a tiny droplet as the main drop passes. This means that particles close to the peaks may not be carried away, but those further away will be plucked out of the surface as in the previous example [30, 31]. In most cases the hydrophobicity of the particle and the surface will prevent water from penetrating between the particle and surface. As the contact line recedes these particles can also be removed by attachment to the drop as liquid will in this case not be left on the surface (Figure 1.8d).

The adhesion between the particle and the solid surface can be a direct adhesion, in which case the surface energies of the two solids are high so bringing them together reduces the

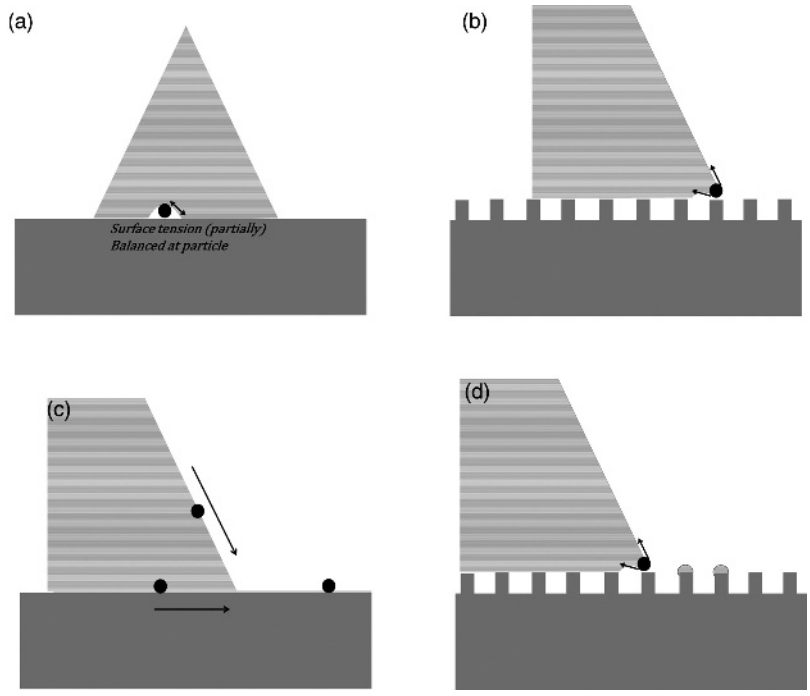

Figure 1.8 *Contact lines receding over different surface types and self-cleaning: (a) Receding into the plane of the page on a flat surface, dirt is trapped; (b) receding to left on Cassie–Baxter surface, surface tension removing particle; (c) receding to left, flat with precursor film, particles in both interfaces remain; (d) receding to left, Cassie–Baxter with film, locally same as (a) but drops/small particles left on protrusions.*

global surface energy. Alternatively, two hydrophobic surfaces can adhere by weaker van der Waals interactions, but if water is present they will be held together by hydrophobic interactions because separation requires wetting of the two interfaces, which would cost surface energy.

For a typical superhydrophobic surface the base material is hydrophobic, meaning that hydrophobic interactions will be important. In this case, as shown in Figure 1.8b, the water would not be expected to wet the crack between the particle and the surface, making removal by the contact line most effective for rolling drops.

A second factor in the removal of particulate material from a roughened surface is the reduction in solid/solid interfacial area. The particles sit on top of small-scale roughness and are not bound strongly because they do not contact a large surface area. The multilayer roughness of the Lotus leaf is important here, the smaller scale roughness prevents particles nesting into crevices and having larger contact areas than on a flat surface.

The third factor is impacting drops – if a surface has different scales of roughness and the instantaneous pressure of the drop impact is only sufficient for it to enter the larger scale of roughness it can collect particles from the crevices of the larger scale roughness.

1.2.2 Other Factors

1.2.2.1 Water Impact

In most cases the water impinging on a self-cleaning superhydrophobic surface will have some momentum. It will either be raindrops or will come from a spray of some kind. In this case there will be a short-lived pressure wave that will push the water into the surface. This could convert the wetting state from bridging Cassie–Baxter to fully wetting Wenzel and, therefore, allow the water to adhere strongly.

If we model the meniscus between some pillars as a vertical capillary we can calculate the pressure required to force liquid to the base as the Laplace pressure.

$$\Delta p = \gamma_{\mathrm{LG}} \left(\frac{1}{R_1} + \frac{1}{R_2} \right) \tag{1.17}$$

The radii required are those of a sphere that forms the advancing angle at the surface of the capillary. For a circular capillary (pore) $R = R_1 = R_2$ and can be calculated from,

$$R = \frac{r}{\cos \theta_{\mathrm{e}}} \tag{1.18}$$

where r is the pore radius, giving

$$\Delta p = \frac{2\gamma_{\mathrm{LG}} \cos \theta_{\mathrm{e}}}{r} \tag{1.19}$$

For a superhydrophobic surface with vertical pillars this penetration resistance pressure can be calculated using the size of the gaps. For multiple layers of roughness the equations above can be used to calculate the effective contact angle on the sides of the pillars. As expected, and as can be seen from the formula, increasing the contact angle and decreasing the pattern size improves the pressure resistance of superhydrophobic surfaces.

A raindrop falling on the surface of a roof will be around 5 mm in diameter and hit the surface at around 9 m s^{-1}. The instantaneous impact pressure has been shown to be a maximum around the periphery of the impact zone, the worst possible case if this area transitions to Wenzel wetting and becomes high hysteresis as the whole drop will then become stuck, the peak pressure is of the order of 4 MPa. For a circular capillary with a contact angle of 180°, using water at standard temperature, the capillary would have to be less than 350 nm in diameter to prevent water from being forced inside. An equivalent triangular lattice of pillars would have a separation of around 300 nm. Using a more realistic contact angle of 100° reduces the critical size to 50 nm and allowing a safety margin reduces it still further. This suggests that the minimum feature size for practical self-cleaning surfaces is quite small and the features must, of course, be able to withstand high impact pressures without damage.

1.2.2.2 Condensation

A further complication is that of condensation inside the roughness. As the surface becomes colder than the air, water condenses directly onto it. In this case it starts in a fully wetting state and often nucleates initially at the base of any roughness, leading to filled patterns, Wenzel wetting and high contact angle hysteresis [32, 33].

This problem is difficult to avoid; theoretically increasing the roughness above a certain level can make the Wenzel wetting state energetically unfavourable, but partial wetting states can still occur, making water adhere strongly to the surface. Very high structures of very small size are fragile. Even with very small features and high aspect ratios it is still possible to become trapped in the Wenzel state. Despite this it has been shown that hierarchically structured surfaces are relatively stable against condensation. Surfaces consisting of layers of fibres are particularly effective as the heat transfer to the substrate is low and water nucleates at the top leaving bridging so the drop can recover. This type of surface is, however, not very good at self-cleaning if the dirt particles penetrate between the fibres and is more suited to water repellence applications. Typically, the Wenzel state and the Cassie–Baxter state of a very rough surface will represent separate energy minima separated by an energy barrier. The energy barrier is present because most partially filled states are higher in energy. The energy barrier can become large, trapping liquid in one state or the other, which becomes a problem if any ever enters the Wenzel fully wetting state as it is then difficult to remove.

Also worth mentioning at this juncture is the Stenocara beetle, which uses local hydrophilic patches to direct condensation, allowing the superhydrophobic part of the surface to remain dry, causing drops of water to grow until the patches cannot hold them, and they then roll to the beetle's mouth [34].

1.2.2.3 Oil Contamination

Surfactants and oils are a serious problem for superhydrophobic self-cleaning surfaces. Oils have relatively low surface tension and are, therefore, more difficult to suspend in a bridging state than water. Likewise, the addition of surfactants to water can reduce the surface tension and therefore the pressure required to penetrate between the features of the roughness, and many surfactants and oils have a high vapour pressure so will not evaporate under normal conditions, making them very difficult to remove [35, 36].

On alkane-based supehydrophobic surfaces oils will super-spread. Their contact angles on flat alkane surfaces are low, so when roughened they decrease to zero; it becomes energetically favourable to cover them with a layer of oil. This is particularly challenging for surfaces that are expected to come into contact with oil, such as vehicle parts and kitchen surfaces. The only solution to this is to use fluorocarbon surfaces with very low surface energies, therefore generating reasonable contact angles with both oils and surfactants, and to enhance this by using highly undercut features to allow liquid to become suspended in the Cassie–Baxter bridging state for contact angles below 90°. This is very successful, but is unlikely to allow technical surfaces to repel oils very effectively due to their cost of fabrication and the fact that once wet with oil through pressure or heat such surfaces are very difficult to clean as the Wenzel state on these surfaces still has a lower energy than the bridging state.

1.2.2.4 Multiple Scale Roughness (Hierarchical Roughness)

The most common way to generate an effective superhydrophobic surface is to use multi-scale roughness. If the smaller scale is small enough to prevent pressure-related penetration

and the larger scale aids rolling, then the surface becomes much more effective than one with a single roughness scale but higher roughness. There are many benefits of using multiple scales.

First, low levels of roughness on several length scales affect each other. Several levels of low angle slopes combined generate overhanging structures, which are particularly effective at promoting water bridging and Cassie–Baxter superhydrophobicity. In this case low levels of roughness can be added together to produce effective superhydrophobic surfaces [37]. This is useful because lower peak sharpness improves the resistance of the structure against friction.

Secondly, in the case of waviness the levels of roughness interact to generate steeper pitches for the liquid to interact with. The obvious example of this was proposed by Herminghaus [38] where a sine wave in two dimensions generates a wavy surface but two overlaid sine waves of very different frequencies generate very steep roughness indeed, even if the amplitude of each one is not that great. In fact the use of multiple layers of roughness is a simple way of generating overhanging roughness. Overhanging roughness can suspend liquids even for contact angles below 90° in a local energy minimum [39].

Thirdly, as mentioned above, multiple level roughness is particularly resistant to pressure wave wetting as well as being more resistant to low surface tension liquids, such as alcohols, and to dew formation [40, 41].

1.2.3 Nature's Answers

Superhydrophobic self-cleaning was first observed on the leaves of the (Indian) Lotus, *Nelumbo nucifera*, which show small wax crystals on the top of waxy bumps. These are highly efficient at self-cleaning and repel a range of water-based liquids, but are sensitive to condensation and physical damage. The wax self-organises on the surface to form nanostructures and microstructures on top of microstructures formed from other components of the leaves in different ways. As described by Koch *et al.* the typical morphologies of these waxes are tubes, prisms and flakes [42].

The self-organised growth of waxes on the leaves means that the plant only needs to exude the waxy mixture and damage to the structures will tend to repair itself [43]. This is a major advantage over artificial surfaces that wear away and become less effective over time. Both the chemistry of the surface and the shape must be maintained to preserve a superhydrophobic effect and waxes are good at both, being able to reorder when warm and dry to hide hydrophilic groups and regenerate surface structure. It has only been possible to copy this in a limited manner so far.

Some other plants and many animals use hair-like structures to generate the roughness required to repel water. This strategy is very effective against condensing water as the water nucleates among the hairs so does not reach the surface. The well known plant Lady's mantle, *Alchemilla mollis*, is thought to use this to collect dew drops on its leaves and allow them to flow to its base. Diving beetles and spiders use a combination of large hairs (setae) and smaller ones (microtrichia). The smaller ones are arranged in a denser array should the larger ones fail for any reason. The hair-like structures are particularly suited to generating persistent air layers underwater, as required by these animals to breathe. The structures have a relatively large area at the interface and a lower area at any other point, making the

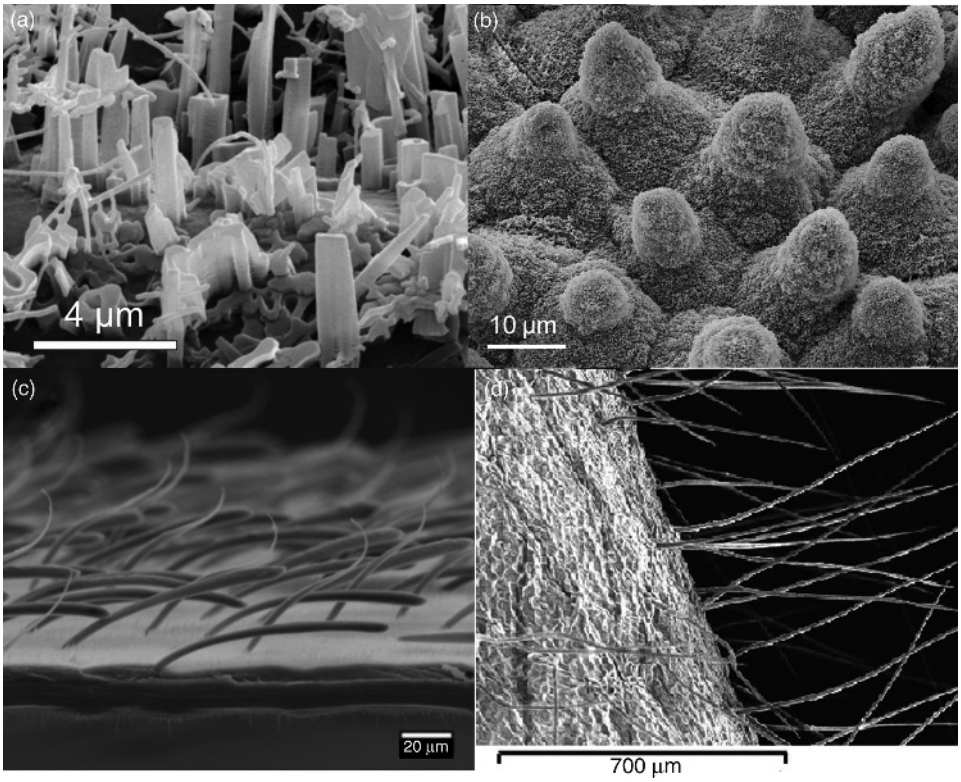

Figure 1.9 *Superhydrophobic structures on various organisms: (a) wax on cabbage, (b) wax on Lotus leaves, (c) bent "hairs" on water boatman Notonecta glauca, (d) Alchemilla Mollis (Ladies Mantle).* Source: *(a) Reproduced with permission from [Ditsche-Kuru et al. Beilstein J Nanotech. 2011, 2, 137–144] Copyright (2011) Beilstein, (b) Reproduced with permission from [] Copyright (2009) American Chemical Society, (c) Reproduced with permission from [Ditsche-Kuru* et al.*, Beilstein J Nanotech. 2011, 2, 137–144] Copyright (2011) Beilstein, open access, (d) Reproduced with permission from [Shirtcliffe et al., Langmuir 2009, 25(24), 14121–14128] Copyright (2009) American Chemical Society.*

surface energy minimum deep and therefore stable. Most aquatic insects achieve this by having structures that come out from their body and then all turn to parallel at the interface, as shown in Figure 1.9c. The second advantage of this system is that there is a degree of elasticity in the structures themselves, so when a pressure wave passes they can move with it and the liquid interface remains attached without slipping deeper into the structure or ejecting gas bubbles [44].

So far these structures have been used less for self-cleaning purposes. Drops become attached to crossing hairs, because the crossing point represents a minimum in energy, and then cannot move very easily. On water insects the structures do not cross because they are all aligned in the same direction so rapid drop movement in one direction and self-cleaning is possible, although if particles penetrated between the structures they would

become difficult to remove as water does not penetrate under normal conditions, unlike on the heirarchical Lotus leaf.

Moth's eyes are structured in a semi-ordered fashion, their primary functions being optical, light gathering and anti-reflection. For these purposes the moth's eyes are structured with conical projections in a hexagonal array. In order for them not to scatter light or to act as lenses they are smaller than the wavelengths of visible light.

This generates a gradient of effective density from the eye to the air and results in very low reflection. There are two huge advantages for the moth, predators do not see the reflection and more light is gathered, helping them to see at night. This type of structure has raised a great deal of interest and ideally would be combined with a self-cleaning function. The obvious use of such a surface would be as a coating on solar cells to reduce scattering and enable self-cleaning. Some artificial surfaces of this type have been designed and show promise although, as with the moth's eyes, the self-cleaning cannot easily be optimised at the same time as the anti-reflectance [45, 46].

Cicadas and other insects use similar structures to repel water from their wings, but they are not as effective as multiscale structures and are unlikely to be self-cleaning without a supporting very small-scale pattern to prevent impinging drops from becoming stuck in the Wenzel state. On the other hand the spiny structures on the feet of water striders for example, *Gerris remingis*, contain nanogrooves and remain dry even after long periods in contact with water. The water strider uses them to glide over the interfacial tension of water bodies, allowing it to collect insects without superhydrophobic surfaces that become captured by it [47].

Butterfly wings also repel water effectively; their wing scales are structured and canted to provide a saw-tooth surface. Experiments show that these structures have a preferred direction for water to move off them [48]. This effect is of potential use in a variety of applications because the pattern can be continued over large areas whereas a pattern of decreasing contact angles could not be. The saw-toothed structure probably generates an uneven contact angle, causing the drop to stick in one direction but roll in the other [49].

The butterfly wing pattern could be used over large areas and drop motion can be driven by gravity or vibration.

Geckos also use soft projections on their feet, but these are spread out at the ends so that they can attach to walls. They function as an extremely compliant surface, enabling close contact with smooth and rough surfaces to maximise surface interactions. The link to superhydrophobicity and self-cleaning is that they must remain clean to function and have been shown to have some self-cleaning properties. Despite adhering strongly to surfaces their surface energy is low and particles are easily transferred from them to most surfaces, in other words they can wipe or walk off particles [50, 51].

1.2.4 Superhydrophilic Self-Cleaning Surfaces

The opposite of superhydrophobicity is superhydrophilicity. In this case the surface energy of the base material is high, causing water to spread out over it, in other words to have a relatively low contact angle. In this case Wenzel's equation can be used to estimate the contact angle that will be observed on the rough surface. Unlike the superhydrophobic case there is no alternative state that takes over at high roughness, so the predicted contact angle soon reaches 0°. Roughness can easily be increased past this point and the question

then is what will happen. The surface wets fully but the rate of wetting inside the roughness of the surface can be more rapid than on a flat surface. Aqil *et al.* [52] showed that the rate of spread of a drop is greater on a rough surface and slows down less as it approaches 0°. In fact the base of the drop can spread so fast that it breaks away from the top, generating a fried-egg shape.

Such surfaces can clean themselves of hydrophobic particles when wet because water enters below the particles and lifts them off as they become attached to the air/water interface. This is also extremely effective against biological contamination but relies on the presence of lots of water [53].

Hydrophilic surfaces are usually strongly adhesive because they have a high surface energy and become coated with material that can bind chemically to them. This can make them very difficult to clean.

Materials with a surface energy the same as that of water can remain very clean when wet because it is energetically favourable for water molecules to sit at the surface. An example of this is polyethylene oxide (PEO) which is used to prevent biofouling in many applications for exactly this reason. The surfaces do not self-clean, but do not become fouled in the first place. If surfaces of this type dry out they can become contaminated and often become damaged because they shrink when dry.

Some self-cleaning products use a combination of superhydrophilic surface properties along with a photocatalyst. The high roughness and hydrophilicity generate a water film when wet and the photocatalyst oxidises organic species to charged species, making surfactants or ultimately completely oxidising them. This combined system allows the surface energy to be higher than that of water with the photocatalysis removing the film of organic matter that spreads over the surface in dry conditions. When wet the high roughness and surface energy causes a water film to lift off the contaminants.

1.2.5 Functional Properties of Superhydrophobic Surfaces

Various routes exist to fabricate superhydrophobic surfaces, allowing a plethora of different material types to be used. Properties inherent in the chosen material can be utilised, for example electrical conductivity, although many other characteristics can be built into materials through the careful design of structure and chemistry. Over the past years attention has moved towards developing advanced materials with properties suitable for a range of applications; either for research or industrial requirements. A number of commercial products making use of superhydrophobicity are already available on the market, with others currently under development. In addition, many patents have been granted for various possible applications of self-cleaning surfaces [54]. Many of these products are used primarily for their superhydrophobic self-cleaning abilities, such as materials used in construction for windows or roofing tiles. Material coatings used in this industry are also widely available, with paints used to form a barrier against bio-fouling or graffiti-resistant layers. The use of non-wettable textiles is also progressing rapidly, with research geared towards identifying methods to modify conventional fabrics and to generate new materials possessing useful functions. These market-led products are mostly driven by novelty, with some products offering better value over existing counterparts in that they have increased functionality [55].

1.2.5.1 Evaporation and Condensation Resistance

The evaporation of liquid drops from solid surfaces has been thoroughly investigated over past decades, although only a few have looked at the interesting phenomena of evaporation from structured superhydrophobic surfaces. On flat solid surfaces two evaporation models were proposed by Picknett *et al.* in 1977: a droplet having diminishing surface contact area with a constant contact angle, or having a constant contact area with a reducing contact angle [56]. For volatile liquid droplets resting on low surface energy substrates the former model was found to be followed when the initial contact angle was $<90^\circ$, giving linear evaporation rates, and when the initial contact angle was $>90^\circ$ the latter model takes precedence, giving non-linear evaporation rates [57]. Xu *et al.* showed how the three-phase contact line of a sessile droplet remains pinned on some superhydrophobic surfaces through the whole evaporation process [58], such that the constant area model is followed. Water resting on the surface of a lotus leaf may penetrate into the roughness, interacting strongly with the natural wax and hindering droplet movement. Most studies examining the effects of liquid evaporation focus on large droplets a few mm in diameter, although condensation onto a surface occurs through the interaction of much smaller droplets. Cheng *et al.* showed experimentally the dramatic difference in wetting characteristics on superhydrophobic lotus leaves, comparing macro-scale water drops to condensation of water from the vapour phase [59]. When wetted with condensing water the high contact angles associated with superhydrophobicity are no longer observed. A more in-depth investigation carried out by McCarthy using topographically patterned silicon pillars as model surfaces gave similar results [60]. During steady condensation, wherein the droplet radius increases proportionally with time, the drop interactions are ultimately important to the dynamics, with droplets coalescing to increase the average droplet size. Baysens *et al.* studied the growth dynamics of condensing water droplets on model surfaces [61] with the initial nucleating droplets being much smaller than feature sizes and forming in between as if they were on planar surfaces. As the drops grow, their initial areas often remain in the fully wetted Wenzel state but new areas covered by coalesced droplets mostly rest in the Cassie–Baxter regime. In their particular case after a very short time ($\sim$1 s) the water was found to move from the slightly wetted features to the more stable Wenzel state, Figure 1.10. Surfaces that go into the Cassie–Baxter state have been proposed for use in condensers because a layer of condensed water at the surface of the cooling pipes is often the limiting factor in condenser design. In the other direction, surfaces that are used for boiling often generate a layer of water vapour at their surface and superhydrophilic surfaces have been suggested for use here to rewet as soon as possible after a bubble forms.

1.2.5.2 Frost/Ice Resistance

Frosting of surfaces can be a serious problem due to changes in surface properties or accumulation of ice or snow. Situations involving reduced friction due to frosting are particularly dangerous, as well as icing of overhead power cables or aeroplane wings, which can result in the failure of electrical insulation or mechanical properties. Bridges are often closed due to the danger of ice falling from supports. Some superhydrophobic surfaces have, however, been shown to reduce freezing temperatures, reduce ice bond strength and even prevent ice formation at their surface [62–64]. Frost formation occurs via two main processes: nucleation and crystal growth, being dependent upon the water

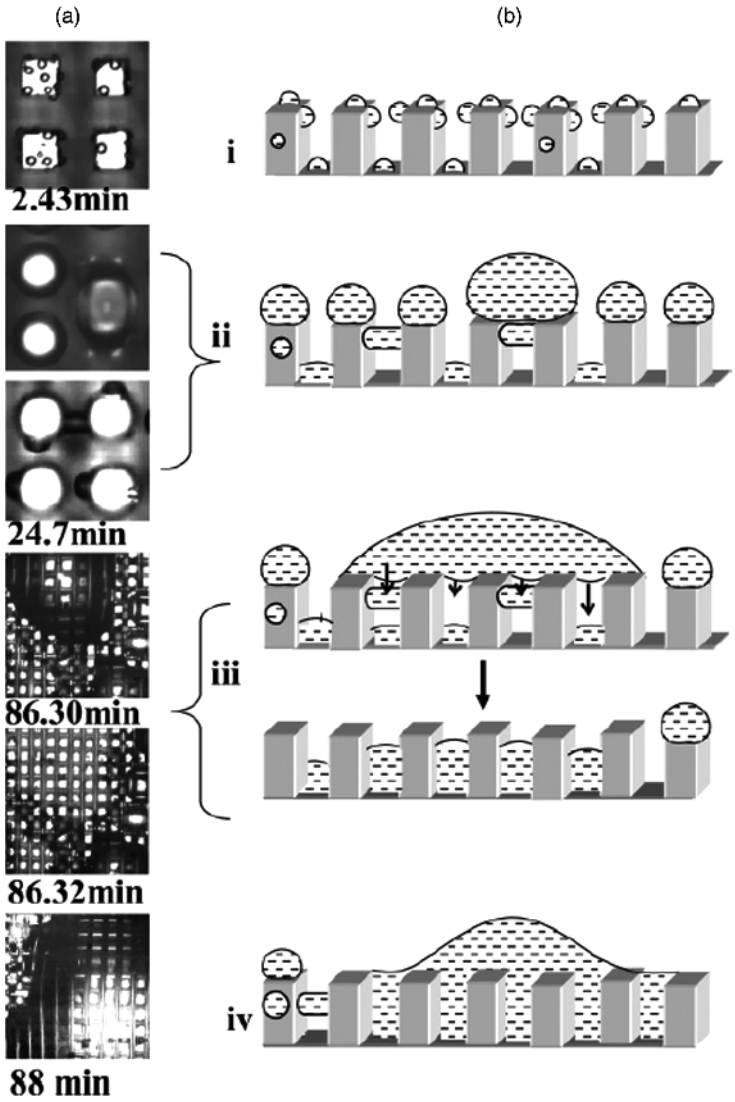

Figure 1.10 *Condensation within structured surfaces [61].* Source: *Reproduced with permission from [Narhe, Langmuir 2007, 23, 6486] Copyright (2007) American Chemical Society.*

vapour overcoming a Gibbs free-energy barrier [65]. Freezing of water has been shown to be significantly delayed when depositing droplets onto cooled superhydrophobic surfaces [66]. Microtextures were found to delay freezing with drops rolling off without leaving behind a film of ice or freezing. Control samples using flat copper showed that slower moving droplets leave a film as they move, which freezes immediately. The low contact area and air gap is thought to reduce the transfer of heat from the liquid to the surface, preventing

freezing. In attempts to mimic natural ice build-up researchers have prepared glazed ice surfaces by spraying super-cooled microdroplets of water onto surfaces held below 0 °C. Kulinich *et al.* investigated the effects of flat versus rough hydrophobic surfaces on the adhesion strength of such ice coatings [67, 68]. Comparison of surfaces based on their contact angle hysteresis showed a direct relationship with adhesion strength. The size of features presented by superhydrophobic surfaces has also been shown to play a role in anti-icing. Using particles with diameters in the range 20 nm to 20 μm. Gao *et al.* showed that larger features gave rise to an increase in the probability of ice formation [69]. Clearly, control over frosting processes is achievable through the use of structured hydrophobic materials. In some cases the superhydrophobic surfaces became damaged by freezing cycles, but a great deal of research is being invested in this area as the potential for ice resistant structures and vehicles is very attractive.

1.2.5.3 Anti-Fouling

Biofouling is the accumulation of biological material on surfaces. Biofouling is a vast area, spanning from problems relating to underwater structures, such as oil-rigs and ship hulls which suffer damage and increased operational and maintenance costs due to accumulation of biomatter, to the medical industry wherein avoiding even small amounts of contamination is paramount. The use of superhydrophobic materials to reduce fouling has been demonstrated through a number of investigations. The main advantage of this approach is that a persistent effect would be expected without releasing chemicals into the environment.

A reduction in the surface area in contact with the liquid carrying the contaminants is often accredited to a reduction in the level of fouling [70], although the shear forces involved in liquid flow and the chemistry presented at the surface have also been shown to impact on protein adsorption/desorption [71]. Koc *et al.* showed that a reduction in the size of features presented at a surface, from micro- to nano-scale, drastically reduced the amount of protein adsorbed, particularly under flow conditions. An initial increase in protein adsorption was observed compared to flat surfaces of the same chemistry, possibly due to slight ingress of the surfactant protein solution into the pores. Others have shown that antifouling can be achieved during short-term exposure, but long term exposure, as would be experienced in a marine environment, gave rise to a gradual deterioration of superhydrophobic surfaces due to fouling [72].

In some cases a similar effect is used where the scale of roughness is set so that the attachment points of a target organism cannot fit the surface and the surface is usually hydrophilic so that water squeezes into the interface and excludes other molecules. This approach is used by some marine organisms [73].

1.2.5.4 Anti-Corrosion

As much as antifouling is important for materials in contact with water, superhydrophobic coatings also present opportunities for use as anti-corrosion treatment. Metals in particular are vulnerable to oxidation, leading to degradation of their mechanical properties. By application of water-repellent materials to their surfaces such breakdown of the metal can

be slowed down or even prevented altogether by preventing the formation of electrochemical cells [74].

Ishizaki *et al.* demonstrated the use of nanostructured cerium oxide films functionalised by fluoroalkylsilanes to protect a magnesium alloy from a corrosive salt solution [75]. The superhydrophobic materials were found to be extremely corrosion resistant, with the adhesion of the overlayer also being shown to be good. Some coatings, however, are not as well adhered to the underlying substrate. Yuan *et al.* demonstrated the use of vinyl modification of copper substrates, from which a fluoropolymer was grafted to form a highly non-wettable and anti-corrosive layer [76]. The copper was first etched to roughen it, with a fluorosilane then being used to form a conformal hydrophobic coating. Electrochemical methods are often used, either to initially roughen surfaces or to deposit coatings. Xu *et al.* used a facile electrochemical machining process to hydrophobise a magnesium alloy, again using a fluorosilane as the chemical modifier [77]. Electrochemical deposition of polypyrrole has been shown to be a rapid and effective means to fabricate relatively good non-wettable surfaces [78]. Within 3 s the zinc could be modified with a 2 μm thick hydrophobic coating having a contact angle of 125°.

Super water-repellent coatings are used in this capacity to exclude liquid water from the metal interface, they have shown positive effect in simple tests, but are seldom suggested as the final external coat due to fragility problems.

1.2.5.5 Transparent and Anti-Reflective Properties

Anti-reflective or optically transparent properties, such as those described for the moth eyes, are sought after in many material and device applications, such as electronic devices, sight correction and sun glasses, lenses and mirrors. Although not a requirement, for many of these possible applications, the ability to self-clean is also a useful capability. One example of particular relevance in the current environmentally-friendly era is the use of transparent, self-cleaning coatings on solar panels. These are not always accessible after installation with maintenance being kept to a minimum by correct selection of surface properties to remain free of dust and to transfer the maximum amount of light to the photocell.

The roughness of the surface is key in terms of the anti-reflection properties as scattering is enhanced by roughness, therefore reducing transparency. For this reason the features required for anti-reflection must be kept smaller than the wavelength of the light that is to be transmitted. When considering visible light this means features should be less than 380–750 nm. Many routes to investigate these properties make use of silica/silicon nanomaterials, with silica nanoparticles being used to impart controlled film thickness and roughness, whilst also allowing ease of chemical modification via silane functionalisation [79, 80]. Silica nanoparticles can be applied as coatings by using charged polymers to attract particle layers. This has been demonstrated by Bravo *et al.* forming transparent films of 20–50 nm silica particles using layer-by-layer deposition of poly(sodium 4-styrenesulfonate) (PSS) and poly(allylamine hydrochloride) (PAH) [81]. By controlling aggregation and layering of the particle layers almost complete visible transparency was achieved, with further chemical modification rendering the surfaces superhydrophobic, Figure 1.11. In most cases anti-reflection is the main function of the layer with water repellency and then self-cleaning being fringe benefits.

Figure 1.11 *Transparent silica nanoparticle superhydrophobic surface [81].* Source: *Reproduced with permission from [Bravo, Langmuir 2007, 23, 7293–7298] Copyright (2007) American Chemical Society.*

These silica nanoparticle surfaces have been shown to demonstrate excellent water repellency as well as antireflective characteristics, and have experimentally shown self-cleaning for 2000 h of outdoor exposure [82].

Polymer coatings have distinct benefits over their inorganic counterparts, being largely flexible and having controllable toughness and stiffness. Researchers have reported an inexpensive method to produce superhydrophobic polymer coatings through *in situ* polymerisation of various monomers [83]. Phase separation of the polymerising solution gave rise to a network of pores in the hydrophobic polymer, giving rise to its non-wettable nature. Altering the composition of the monomer mixture gave control over surface morphology from nano- to micro-roughness, whilst photografting was used to adjust the surface chemistry. Transparent films were afforded by a reduction in the architecture to nanoscale features.

1.3 Materials and Fabrication

As discussed above there are many examples of superhydrophobicity in nature, having wide-ranging applications from self-cleaning to liquid harvesting. Synthetic methods to mimic such surfaces have been developed making use of many different types of materials, allowing a range of properties of the final surface. The required characteristics are that the surface must be rough, of the order of nano- to microscale and present a hydrophobic chemistry. Dual-scale roughness is advantageous to form surfaces having both high water contact angles and low sliding angles [84]. The material itself could be inherently hydrophobic, with this being roughened to form a simple superhydrophobic surface – such as roughening a poly(tetrafluoroethylene) (PTFE) plate [85]. If the material is not chemically hydrophobic, then a chemical coating is normally added after the surface structure is formed, as in the case of fluoro/alkylsilane treatment often used to form many reported superhydrophobic materials. Other methods produce a coating that presents both the structure and the chemistry required.

Since the early 1940s researchers have been interested in the wetting properties of surfaces, with more and more focus on the applications of such knowledge being brought about by technology and industrial applications of the 1990s. The number of methods reported in the literature to produce materials/ surfaces/ coatings presenting superhydrophobic properties has increased substantially over the past decade, with endless strategies demonstrating potential for scale-up of materials processing.

The careful control over etching processes can lead to degradation of polymers such that they are morphologically altered. High-energy oxygen species present in gas-phase plasmas have been used to etch fluorinated polymers to create surfaces with water contact angles of ∼170° [86]. Similar methods have been used to roughen many polymers, such as polypropylene [87]. Ellinas *et al.* used colloidal lithography of polystyrene to mask off a polymethylmethacrylate (PMMA) sheet before etching with an oxygen-plasma, as shown in Figure 1.12 [88]. Polymer microbeads were spin-coated onto the substrate to form highly ordered structures to pattern the surface. A similar approach was also used to selectively etch silicon substrates to form features with very high aspect-ratios.

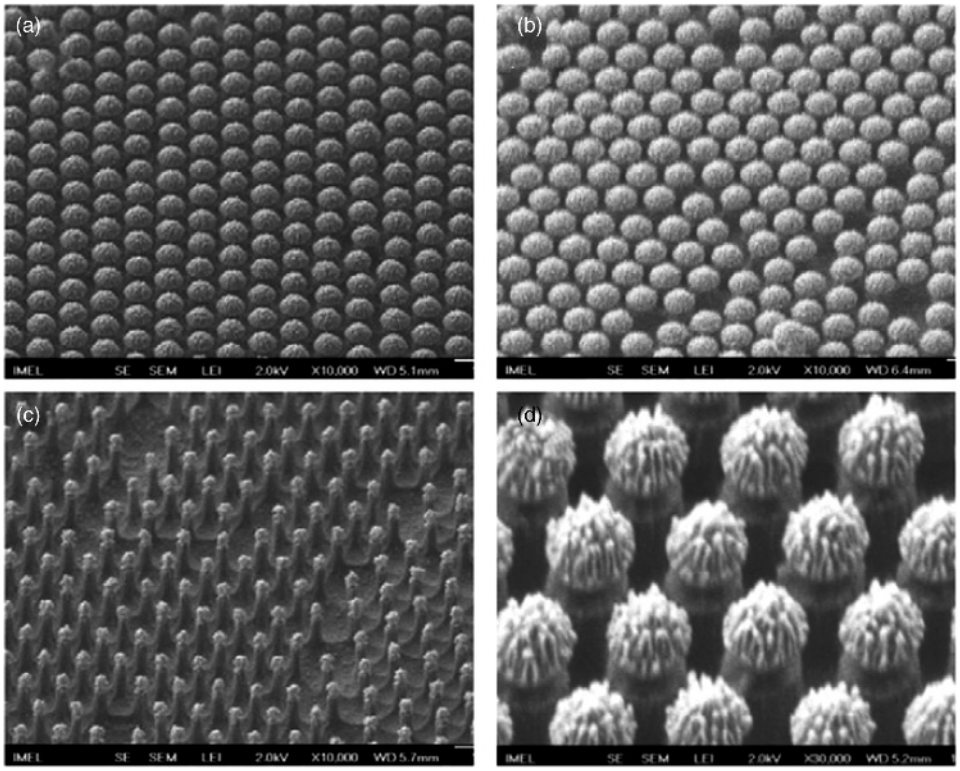

Figure 1.12 *PMMA pillar arrays produced via plasma etching: (a) −60 V bias, 1 min etch; (b) –80 V bias, 1 min etch; (c) −60 V bias, 2 min etch; (d) −80 V bias, 1 min etch.* Source: *Adapted with permission from [Ellinas, Microelectronic Eng. 2011, 88, 2547–2551] Copyright (2011) Elsevier.*

Langmuir–Blodgett deposition of micro- and nano-scale silica particles is also commonly used to present ordered features, with the structures usually being rendered hydrophobic by post modification with a hydrophobic silane [89].

Phase-separation of polymers can lead to the micro-/nano-scale features required for superhydrophobicity. This method of modification is carried out *in-situ* with a surface coating being formed. Hydrophobic phase-separation of sol–gel based solutions has afforded superhydrophobic materials which display very high water contact-angles [90]. Polymers are more often used, in part due to their flexibility leading to greater durability. A copolymer equimolar in fluorinated acrylate and methyl methacrylate monomers has been shown to produce hexagonally-packed nano-scale pores during drying under strictly controlled humidity conditions [91]. Through fine-tuning of both the size of these pores and the thickness of the deposited film the coating can present superhydrophobicity and be optically transparent.

Electrodeposition under diffusion limited conditions is also commonly used for the fabrication of rough structures. Various TiO_2 nanostructures can be formed on titanium surfaces. Lai *et al.* prepared nano-pore, nano-tube and nano-vesuvianite structures, which could be used to alter water contact modes at the nanometre scale [92]. Anodization of aluminum gives rise to porous membranes, which can be further chemically treated to form superhydrophobic surfaces [93].

Many other methods are available making use of a range of materials. Although early work looked mainly at textiles or wax-based materials, more recent work has been driven to examine potential modification strategies for metals. Through a two-pronged approach researchers are looking to develop robust methods to produce durable superhydrophobic properties via cost-effective routes, either by direct roughening of inherently hydrophobic materials or, more widely, by adding an overlayer to alter the outermost layer of the materials. A number of recent reviews cover the fabrication of superhydrophobic materials/ coatings in depth [94–96].

1.4 Future Perspectives

Through our inspiration from nature we now look to mimic the properties of surfaces that surround us in order to improve our innovations and technologies. Over the past decades we have advanced our understanding of the interface between liquids and solids such that we can now design and fabricate surfaces to exhibit specific properties, alone or in combination, such as water repellency and anti-fouling/ anti-corrosion. These have either been driven by fundamental research or the need for new coatings, such as advances in photocells as well as advances in micro-structuring technology.

Applications for superhydrophobic materials are widespread, only really limited by the cost and fragility of typical superhydrophobic surfaces. Outdoor weather-proof paints, easy-clean textiles and self-cleaning glass used for windows of apartment or office block skyscrapers are all examples of how superhydrophobicity is used in our surroundings. Superhydrophilicity, the flip side of the coin, is used in self-cleaning windows and roof tiles and also in mist-free mirrors, causing the condensed water to spread to a film and also remove some contamination. Technologies within laboratory settings are also being improved. Lab-on-a-chip devices of interest to a multi-disciplinary audience for the miniaturisation

and development of high-throughput processes are possibly the next application to be advanced by the incorporation of superhydrophobic surfaces. Clinical diagnostic devices making use of such technologies may benefit from an enhancement in device longevity and sensitivity of analyte detection through the anti-fouling capabilities of superhydrophobic and superhydrophilic surfaces.

Our ability to prepare complicated surfaces structured on a micro- and nano-scale has improved massively in the last few years and has enabled various technologies to advance from the laboratory into the real world as their cost has fallen to a level where application is possible. The development and production of both random roughness and more advanced sculptured surfaces has resulted in both simple and advanced self-cleaning surfaces becoming available. The combination of superhydrophobicity and other properties, such as anti-reflection or ice protection, is possible, although the optimum topography and chemistry of the surface will often be specific for the application.

References

1. Lotus Effect® was trademarked in 1998 by W. Barthlott and his colleagues.
2. Roach, P., Shirtcliffe, N. and Newton, M. (2008) Progress in superhydrophobic surface development. *Soft Matter*, **4**, 224–240.
3. Extrand, C. (2006) *Encyclopedia of Surface and Colloid Science*, 2nd edn (ed. P. Somasundaran), Taylor and Francis, New York, pp. 5854–5868.
4. Bhusan, B. and Jung, Y. (2011) Superhydrophobicity, self-cleaning, low adhesion, and drag reduction. *Prog. Mater. Sci.*, **56**, 1–108.
5. Guo, Z., Liu, W. and Su, B. (2011) Superhydrophobic surfaces : From natural to biomimetic to functional. *J. Colloid Interface Sci.*, **353**, 335–355.
6. Genzer, J. and Marmur, A. (2008) Biological and synthetic self- cleaning surfaces. *MRS Bull.*, **33**, 742–746.
7. Ma, M., Hill, R. and Rutledge, G. (2008) A review of recent results on superhydrophobic materials based on micro- and nanofibers. *J. Adhes. Sci. Technol.*, **22**, 1799–1817.
8. Extrand, C. (2006) *Encyclopedia of Surface and Colloid Science* (ed. P. Somasundaran), Taylor and Francis, New York, pp. 5854–5868.
9. Young, T. (1805) An essay on the cohesion of fluids. *Philos. Trans. R. Soc. London*, **95**, 65.
10. de Gennes, P. (1895) Wetting: Statics and dynamics. *Rev. Mod. Phys.*, **57** (3): 827–863.
11. Fabretto, M., Sedev, R. and Ralston, J. (2003) *3rd International Symposium on Contact Angle, Wettability and Adhesion*, vol. **3** (ed. K.L. Mittal, VSP International Science Publishers, pp. 161–173.
12. Olsen, D.A., Joyner, P.A. and Olson, M.D. (1962) Sliding of water drops on microstructured hydrophobic surfaces. *J. Phys. Chem.*, **66** (5), 883–886.
13. Furmidge, C.G.L. (1962) Studies at phase interfaces. I. The sliding of liquid drops on solid surfaces and a theory for spray retention. *J. Colloid Sci.*, **17**, 309.
14. Shanahan, M.E.R. and DeGennes, P.G. (1986) The ridge produced by a liquid near the triple line solid liquid fluid. *Compt. Rend. Ser. II*, **302**, 517.
15. Gao, L. and McCarthy, T. (2008) Teflon is hydrophilic. Comments on definitions of hydrophobic, shear versus tensile hydrophobicity, and wettability characterization. *Langmuir*, **24**, 9183–9188.

16. De Souza, E., Gao, L., McCarthy, T. *et al.* (2008) Effect of contact angle hysteresis on the measurement of capillary forces. *Langmuir*, **24**, 1391–1396.
17. Wenzel, R.N. (1936) Resistance of solid surfaces to wetting by water. *Ind. Eng. Chem.*, **28**, 988–994.
18. Cassie, A.B.D. and Baxter, S. (1944) Wettability of porous surfaces. *Trans. Faraday Soc.*, **40**, 546.
19. De Gennes, P., Brochard-Wyart, F. and Quere, D. (2003) *Capillarity and Wetting Phenomena: Drops, Bubbles, Pearls, Waves*, Springer.
20. Quere, D., Lafuma, A. and Bico, J. (2003) Slippy and sticky microtextured solids. *J. Nanotech.*, **14**, 10.
21. Gao, L. and McCarthy, T. (2007) How Wenzel and Cassie were wrong. *Langmuir*, **23** (7), 3762–3765.
22. McHale, G. (2007) Cassie and Wenzel: Were they really so wrong? *Langmuir*, **23** (15), 8200–8205.
23. Panchagnula, M. and Vedantam, S. (2007) Comment on how Wenzel and Cassie were wrong by Gao and McCarthy. *Langmuir*, **23** (26), 13242.
24. Gao, L. and McCarthy, T. (2009) An attempt to correct the faulty intuition perpetuated by the Wenzel and Cassie "Laws". *Langmuir*, **25** (13), 7249–7255.
25. Quere, D. (2002) Surface chemistry: Fakir droplets. *Nature Mater.*, **1**, 14.
26. Patankar, N. (2004) Transition between superhydrophobic states on rough surfaces. *Langmuir*, **20**, 7097.
27. Reyssat, M., Yeomans, J. and Quere, D. (2008) Impalement of fakir drops. *Europhys. Lett.*, **81**, art. 26006.
28. Dorrer, C. and Ruhe, J. (2007) Condensation and wetting transitions on microstructured ultrahydrophobic surfaces. *Langmuir*, **23** (7), 3820–3824.
29. Barthlott, W. and Neinhuis, C. (1997) Purity of the sacred lotus, or escape from contamination in biological surfaces. *Planta*, **202** (1), 1–8.
30. Krumpfer, J., Bian, P., Zheng, P. *et al.* (2011) Contact angle hysteresis on superhydrophobic surfaces: An ionic liquid probe fluid offers mechanistic insight. *Langmuir*, **27** (6), 2166–2169.
31. Krumpfer, J. and McCarthy, T. (2011) Dip-coating crystallization on a superhydrophobic surface: A million mounted crystals in a 1 cm2 array. *J. Am. Chem. Soc.*, **133** (15), 5764–5766.
32. Bico, J., Marzolin, C. and Quere, D. (1999) Pearl drops. *Europhys. Lett.*, **47** (2), 220–226.
33. Mockenhaupt, B., Ensikat, H., Spaeth, M. and Barthlott, W. (2008) Superhydrophobicity of Biological and Technical Surfaces under Moisture Condensation: Stability in Relation to Surface Structure. *Langmuir*, **24** (23), 13591–13597.
34. Parker, A.R. and Lawrence, C.R. (2001) Water capture by a desert beetle. *Nature*, **414** (6859), 33–34.
35. Milne, A.J.B., Elliott, J.A.W., Zabeti, P. *et al.* (2011) Model and experimental studies for contact angles of surfactant solutions on rough and smooth hydrophobic surfaces. *Phys. Chem. Chem. Phys.*, **13**, 16208–16219.
36. Ferrari, M., Ravera, F., Rao, S. and Liggieri, L. (2006) Surfactant adsorption at superhydrophobic surfaces. *Appl. Phys. Lett.*, **89**, 053104.
37. Shirtcliffe, N., McHale, G., Newton, M. *et al.* (2004) Dual-scale roughness produces unusually water-repellent surfaces. *Adv. Mater.*, **16** (21), 1929–1932.

38. Herminghaus, S. (2000) Roughness-induced non-wetting. *Europhys. Lett.*, **52**, 165.
39. Tuteja, A., Choi, W., Ma, M. *et al.* (2007) Designing superoleophobic surfaces. *Science*, **318**, 1618–1622.
40. Cheng, Y., Rodak, D., Wong, C. and Hayden, C. (2006) Effects of micro- and nano-structures on the self-cleaning behaviour of lotus leaves. *Nanotechnology*, **17** (5), 1359–1362.
41. Nosonovsky, M. (2007) Multiscale roughness and stability of superhydrophobic biomimetic interfaces. *Langmuir*, **23** (6), 3157–3161.
42. Koch, K., Bohn, F. and Barthlott, W. (2009) Hierarchically sculptured plant surfaces and superhydrophobicity. *Langmuir*, **25** (24), 14116–14120.
43. Koch, K., Dommisse, A., Niemietz, A. *et al.* (2009) Nanostructure of epicuticular plant waxes: Self-assembly of wax tubules. *Surf. Sci.*, **603**, 1961–1968.
44. Flynn, M.R. and Bush, W.M. (2008) Underwater breathing: The mechanics of plastron respiration. *J. Fluid Mech.*, **608**, 275–296.
45. Xiu, Y., Zhang, S., Yelundur, V. *et al.* (2008) Superhydrophobic and low light reflectivity silicon surfaces fabricated by hierarchical etching. *Langmuir*, **24**, 10421–10426.
46. Park, Y., Im, H., Im, M. and Choi, Y. (2011) Self-cleaning effect of highly water-repellent microshell structures for solar cell applications. *J. Mater. Chem.*, **21**, 633–636.
47. Gau, X. and Jiang, L. (2004) Biophysics: Water-repellent legs of water striders. *Nature*, **432**, 36.
48. Zheng, Y., Gao, X. and Jiang, L. (2007) Directional adhesion of superhydrophobic butterfly wings. *Soft Matter*, **3**, 178–182.
49. Kusumaatmaja, H. and Yeomans, J. (2009) Anisotropic hysteresis on ratcheted superhydrophobic surfaces. *Soft Matter*, **5**, 2704–2707.
50. Hansen, W.R. (2005) Evidence for self-cleaning in gecko setae. *PNAS*, **102**(2), 385–389.
51. Autumn, K. and Hansen, W. (2006) Ultrahydrophobicity indicates a non-adhesive default state in gecko setae. *J. Comp. Physiol.*, **192**, 1205–1212.
52. McHale, G., Shirtcliffe, N., Aqil, S. *et al.* (2004) Topography driven spreading. *Phys Rev Lett.*, **93**(3),036102.
53. Genzer, J. and Efimienko, K. (2006) Recent developments in superhydrophobic surfaces and their relevance to marine fouling: A review. *Biofouling*, **22** (5), 339–360.
54. Nosonovsky, M. and Bhushan, B. (2008) *Multiscale Dissipative Mechanisms and Hierarchical Surfaces-Friction, Superhydrophobicity, and Biomimetics*, Springer, New York.
55. Blossey, R. (2003) Self-cleaning surfaces – virtual realities. *Nat. Mater.*, **2**, 301–306.
56. Picknett, R.G. and Bexon, R. (1977) Evaporation of sessile or pendant drops in still air. *J. Colloid Interface Sci.*, **61**, 336–350.
57. Birdi, K.S., Vu, D.T. and Winter, A. (1989) A study of the evaporation rates of small water drops placed on a solid-surface. *J. Phys. Chem.*, **93**, 3702–3703.
58. Zhang, X.Y., Tan, S.X., Zhao, N. *et al.* (2006) Evaporation of sessile water droplets on superhydrophobic natural lotus and biomimetic polymer surfaces. *ChemPhysChem.*, **7**, 2067–2070.
59. Cheng, Y.T. and Rodak, D.E. (2005) Is the lotus leaf superhydrophobic? *Appl. Phys. Lett.*, **86**, 144101.

60. Wier, K.A. and McCarthy, T.J. (2006) Condensation on ultrahydrophobic surfaces and its effect on droplet mobility: Ultrahydrophobic surfaces are not always water repellant. *Langmuir*, **22**, 2433–2436.
61. Narhe, R.D. and Beysens, D.A. (2007) Growth dynamics of water drops on a square-pattern rough hydrophobic surface. *Langmuir*, **23**, 6486–6489.
62. Nakajima, A., Hashimoto, K. and Watanabe, T. (2001) Recent studies on super-hydrophobic films. *Monatsh. Chem.*, **132**, 31–41.
63. Sarkar, D.K. and Farzaneh, M. (2009) Superhydrophobic coatings with reduced ice adhesion. *J. Adhesion Sci. Technol.*, **23**, 1215–1237.
64. Menini, R. and Farzaneh, M. (2009) Elaboration of Al(2)O(3)/PTFE icephobic coatings for protecting aluminum surfaces. *Surf. Coat. Technol.*, **203**, 1941–1946.
65. Fletcher, N.H. (2009) *The Chemical Physics of Ice*, Cambridge University Press, Cambridge.
66. Tourkine, P., Le Merrer, M. and Quéré, D. (2009) Delayed freezing on water repellent materials. *Langmuir*, **25**, 7214–7216.
67. Kulinich, S.A. and Farzaneh, M. (2004) Alkylsilane self-assembled monolayers: Modeling their wetting characteristics. *Appl. Surf. Sci.*, **230**, 232–240.
68. Kulinich, S.A. and Farzaneh, M. (2009) Ice adhesion on super-hydrophobic surfaces. *Appl. Surf. Sci.*, **255**, 8153–8157.
69. Cao, L.L., Jones, A.K., Sikka, V.K. *et al.* (2009) Anti-Icing Superhydrophobic Coatings. *Langmuir*, **25**, 12444–12448.
70. Marmur, A. (2006) Super-hydrophobicity fundamentals: Implications to biofouling prevention. *Biofouling*, **22**, 107–115.
71. Koc, Y., de Mello, A.J., McHale, G. *et al.* (2008) Nanoscale superhydrohobicity: Suppression of protein adsorption and promotion of flow induced detachment. *Lab Chip*, **8**, 582–586.
72. Zhang, X., Shi, F., Niu, J. *et al.* (2008) Superhydrophobic surfaces: From structural control to functional application. *J. Mater. Chem.*, **18**, 621–633.
73. Callow, J. and Callow, M. (2011) Trends in the development of environmentally friendly fouling-resistant marine coatings. *Nature Commun.*, **2**. doi: 10.1038/ncomms 1251
74. Barkhudarov, P.M., Shah, P.B., Watkins, E.B. *et al.* (2008) Corrosion inhibition using superhydrophobic films. *Corros. Sci.*, **50**, 897–902.
75. Ishizaki, T., Masuda, Y. and Sakamoto, M. (2011) Corrosion resistance and durability of superhydrophobic surface formed on magnesium alloy coated with nanostructured cerium oxide film and fluoroalkylsilane molecules in corrosive NaCl aqueous solution. *Langmuir*, **27**(8), 4780–4788.
76. Yuan, S.J., Pehkonen, S.O., Liang, B. *et al.* (2011) Superhydrophobic fluoropolymer-modified copper surface via surface graft polymerisation for corrosion protection. *Corros. Sci.*, **53** (9), 2738–2747.
77. Xu, W., Song, J., Sun, J. *et al.* (2011) Rapid fabrication of large-area, corrosion-resistant superhydrophobic Mg alloy surfaces. *ACS Appl. Mater. Interfaces*, **3** (11), 4404–4414.
78. Hermelin, E., Petitjean, J., Lacroix, J.C. *et al.* (2008) Ultrafast electrosynthesis of high hydrophobic polypyrrole coatings on a zinc electrode: Applications to the protection against corrosion. *Chem. Mater.*, **20**, 4447–4456.

79. Li, Y., Liu, F. and Sun, J.Q. (2009) A facile layer-by-layer deposition process for the fabrication of highly transparent superhydrophobic coatings. *Chem. Commun.*, 2730–2732.
80. Deng, X., Mammen, L., Zhao, Y. *et al.* (2011) Transparent, thermally stable and mechanically robust superhydrophobic surfaces made from porous silica capsules. *Adv. Mater.*, **23** (26), 2962–2965.
81. Bravo, J., Zhai, L., Wu, Z. *et al.* (2007) Transparent superhydrophobic films based on silica nanoparticles. *Langmuir*, **23**, 7293–7298.
82. Manca, M., Cannavale, A., De Marco, L. *et al.* (2009) Durable superhydrophobic and antireflective surfaces by trimethylsilanized silica nanoparticles-based sol-gel processing. *Langmuir*, **25**, 6357–6362.
83. Levkin, P.A., Svec, F. and Frechet, J.M.J. (2009) Porous polymer coatings: A versatile approach to superhydrophobic surfaces. *Adv. Funct. Mater.*, **19**, 1993–1998.
84. Gao, L. and McCarthy, T.J. (2006) The "lotus effect" explained: Two reasons why two length scales of topography are important. *Langmuir*, **22**, 2966–2967.
85. Zhang, J.L., Li, J.A. and Han, Y.C. (2004) Superhydrophobic PTFE surfaces by extension. *Macromol. Rapid. Commun.*, **25**, 1105–1108.
86. Shiu, J.-Y., Kuo, C.-W. and Chen, P. (2005) Fabrication of tunable superhydrophobic surfaces. *Proc. SPIE*, **5648**, 325–332.
87. Youngblood, J.P. and McCarthy, T.J. (1999) Ultrahydrophobic polymer surfaces prepared by simultaneous ablation of polypropylene and sputtering of poly(tetrafluoroethylene) using radio frequency plasma. *Macromolecules*, **32**, 6800–6806.
88. Ellinas, K., Smyrnakis, A., Malainou, A. *et al.* (2011) "Mesh-assisted" colloidal lithography and plasma etching: A route to large-area, uniform, ordered nano-pillar and nanopost fabrication on versatile substrates. *Microelectron. Eng.*, **88**, 2547–2551.
89. Szu, P.S., Yang, Y.M. and Lee, Y.L. (2007) Hierarchically structured superhydrophobic coatings fabricated by successive Langmuir-Blodgett deposition of micro-/nano-sized particles and surface silanization. *Nanotechnology*, **18**, 465604.
90. Shirtcliffe, N.J., Mchale, G., Newton, M.I. *et al.* (2005) Porous materials show superhydrophobic to superhydrophilic switching. *Chem. Commun.*, **25**, 3135–3137.
91. Yabu, H. and Shimomura, M. (2005) Single-step fabrication of transparent superhydrophobic porous polymer films. *Chem. Mater.*, **17**, 5231–5234.
92. Lai, Y.K., Gao, X.F., Zhuang, H.F. *et al.* (2009) Designing superhydrophobic porous nanostructures with tunable water adhesion. *Adv. Mater.*, **21**, 3799–3803.
93. Shibuichi, S., Onda, T., Satoh, N. and Tsujii, K. (1996) Super water-repellent surfaces resulting from fractal structure. *J. Phys. Chem.*, **100**, 19512–19517.
94. Yan, Y.Y., Gao, N. and Barthlott, W. (2011) Mimicking natural superhydrophobic surfaces and grasping the wetting process: A review on recent progress in preparing superhydrophobic surfaces. *Adv. Colloid Interface Sci.*, **169**, 80–105.
95. Liu, K.S. and Jiang, L. (2011) Bio-inspired design of multiscale structures for function integration. *Nano Today*, **6** (2), 155–175.
96. Guo, Z.G., Liu, W.M. and Su, B.L. (2011) Superhydrophobic surfaces: From natural to biomimetic to functional. *J. Colloid Interface Sci.*, **353** (2), 335–355.